ISSN: 3106-0668
e-ISSN: 3104-4700

JOURNAL OF MEDICINE-24

JOURNAL OF
MEDICINE–24

Volume: 3 Issue: 2

2026

International Indexing

© medicine24@aem.az
© info@aem.az
© aem.az/en

Journal of MEDICINE–24
August 2026, Volume 3, Issue 2, pp. 4−10
DOI: https://doi.org/10.36719/3104-4700/5/4-10

Predictive Modeling of Cognitive Decline in Alzheimer's Disease via Multi-Modal Digital Twins: Algorithmic Limitations, Explainable AI, and Healthcare Management Perspectives

Elcin Huseyn

Abstract. *The heterogeneous progression of Alzheimer's disease (AD) continuously challenges the boundaries of traditional clinical neurology, particularly in early diagnosis and the personalized administration of disease-modifying therapies. In recent years, the paradigm of the "digital twin" a dynamic, data-driven in silico replica of a patient's neurobiological profile, has emerged as a theoretical solution to this heterogeneity. Despite its growing prominence in computational neuroscience, the current literature reveals significant methodological fragmentation regarding data fusion strategies and algorithmic architectures. This critical review synthesizes recent advancements (2020–2025) in multi-modal digital twin models aimed at predicting cognitive attrition in AD. We critically analyze the limitations of unimodal biomarker reliance and the polarizing debate between ensemble learning methods and Deep Neural Networks (DNNs). Our synthesis indicates that while Deep Learning achieves superior diagnostic accuracy in spatial topography, its inherent algorithmic opacity ("black box" phenomenon) severely undermines clinical utility and trust. Furthermore, we evaluate the implementation of these models through the lens of healthcare management, emphasizing how predictive simulations can optimize resource allocation and transform health policy. We conclude that the future of neurodegenerative care relies not merely on algorithmic complexity, but on the integration of Explainable Artificial Intelligence (XAI) to support transparent, multi-modal clinical decision-making.*

Keywords: *digital twin, Alzheimer's disease, cognitive decline, computational neuroscience, Explainable AI, multi-modal data fusion, healthcare management*

Introduction

The Clinical Impasse and the Digital Twin Paradigm

The global demographic shift toward an aging population has positioned neurodegenerative disorders, predominantly Alzheimer's disease (AD), as one of the most critical challenges facing modern healthcare systems. The fundamental pathophysiological cascade of AD-characterized by the accumulation of amyloid-beta (Aβ) plaques and intracellular neurofibrillary tangles of hyperphosphorylated tau-often precedes clinical manifestations by decades (Jack et al., 2018).

World Health, Medical and Life Sciences Organization, Dr. Neuroscience, Rotterdam, Netherlands
E-mail: elcin.huseyn@whml.org
Received: 9 April 2026; Accepted: 13 July 2026; Published online: 15 August 2026

However, the spatiotemporal progression of these protein apathies, and the resulting cognitive decline, exhibit profound inter-individual variability. Traditional neurological protocols, heavily reliant on cross-sectional neuroimaging and periodic cognitive assessments (e.g., MoCA, MMSE), function reactively. This "one-size-fits-all" diagnostic approach fails to capture the dynamic temporal nuances of neurodegeneration, leading to delayed interventions, suboptimal therapeutic efficacy, and a substantial strain on healthcare infrastructure.

To overcome the limitations of reactive medicine, the concept of the "digital twin" originally conceptualized in aerospace and systems engineering for predictive maintenance-has been increasingly adopted within computational neuroscience (Coorey et al., 2022). In the context of neurodegeneration, a digital twin represents a virtual, computationally dynamic replica of a patient. It is continuously updated with multi-modal patient data, including genomic profiles, fluid biomarkers, neuroimaging, and real-time physiological metrics. By simulating the complex biological mechanisms of the central nervous system, these models attempt to forecast the trajectory of synaptic loss and the subsequent degradation of human decision-making pathways long before clinical thresholds are breached (Popuri et al., 2020).

Despite an exponential increase in literature surrounding medical digital twins, a critical examination reveals severe methodological inconsistencies. Current discourse is sharply divided into optimal data fusion techniques and the choice of underlying machine learning architectures (Garrison et al., 2021). The objective of this paper is to move beyond a mere descriptive summary of recent literature. Instead, we provide a critical synthesis of the algorithmic boundaries governing AD digital twins, evaluating their true clinical validity, the necessity for algorithmic transparency, and their broader implications for healthcare management and policy execution (Topol, 2025).

Methodology of the Review

A comprehensive literature search was conducted utilizing PubMed, Scopus, and the Web of Science core collections, restricting the publication window to the last five years (2020–2025) to capture the most contemporary computational paradigms. The search strategy was highly specified using Boolean operators: ("digital twin" OR "computational simulation") AND ("Alzheimer's disease" OR "cognitive decline") AND ("machine learning" OR "multi-modal data fusion").

Initial screening yielded 412 articles. To maintain methodological rigor, studies that were purely conceptual, lacked empirical algorithmic validation, or relied on synthetic data without clinical cohort grounding (e.g., ADNI, OASIS, or local hospital cohorts) were excluded. The final thematic synthesis comprises 48 peer-reviewed articles, clinical trial reports, and meta-analyses. The selected studies were critically evaluated based on three parameters: (a) the complexity of their multi-modal data integration, (b) the architectural transparency of their predictive algorithms, and (c) their translational viability into clinical workflow and healthcare administration.

The Landscape of Multi-Modal Data Fusion: Literature Synthesis and Contradictions

The fundamental premise of a digital twin relies on its ability to mirror the physiological state of its physical counterpart. In AD modeling, this requires the integration of highly heterogeneous data types. A critical review of the literature reveals a significant divide between unimodal and multi-modal fusion strategies.

The Fallacy of Unimodal Projections

Early iterations of computational neuro-modeling heavily favored unimodal approaches, predominantly utilizing structural Magnetic Resonance Imaging (sMRI). For instance, studies by

Wang et al. (2023) utilized morphological feature extraction to predict cortical thinning, achieving high specificity in mapping anatomical degradation. However, from a critical standpoint, relying solely on sMRI represents a static snapshot of end-stage cellular death (Alhaddad & O'Brien, 2023). It fails to account for the upstream biochemical alterations that drive the disease. Consequently, unimodal models consistently demonstrate a high error rate when attempting to predict *when* a patient transitioning from Mild Cognitive Impairment (MCI) will experience a precipitous drop in executive function and decision-making capabilities.

Synergistic Multi-Modal Architectures
More recent and robust paradigms advocate for multi-modal data fusion, combining genotypic risk factors (e.g., APOE-ε4 allele presence), cerebrospinal fluid (CSF) or plasma biomarkers (p-tau181, Aβ42/40 ratio, Neurofilament light chain [NfL]), and neuroimaging (FDG-PET and sMRI) (Teipel & Grothe, 2020). Koutsouleris and Friston (2021) demonstrated that integrating physiological biomarkers with structural data drastically improves the prognostic timeline, allowing algorithms to forecast cognitive attrition up to 24 months in advance (Redekop & Mladsi, 2024).

Critical Synthesis
The literature suggests a clear consensus that multi-modal fusion is biologically superior. However, the exact mathematical methodology of this fusion remains highly experimental. "Early fusion" techniques often lead to the "curse of dimensionality," where the noise of unstructured data overwhelms the signal. Conversely, "late fusion" techniques often fail to capture the critical non-linear interactions between genetic polymorphism and subsequent regional brain atrophy. Literature urgently requires standardized, biologically informed fusion frameworks rather than purely mathematical concatenations.

Deep Dive into Algorithmic Architectures: The Mathematical Modeling of Neurodegeneration

The translation of biological phenomena into a digital twin necessitates algorithmic frameworks capable of handling high-dimensional, non-linear, and longitudinally sparse datasets. In modeling Alzheimer’s disease, the computational challenge is mapping the trajectory from localized proteinopathy to macroscopic systemic failure.

Ensemble Learning and Decision Trees: The Case for Random Forests

For highly structured, tabular clinical datasets, ensemble learning remains the gold standard. Random Forest (RF) and Extreme Gradient Boosting (XGBoost) algorithms construct robust predictive models by aggregating the outputs of hundreds or thousands of independent decision trees (Fisher et al., 2024).

The mathematical strength of Random Forests in neurodegeneration lies in "bootstrap aggregating" (bagging). By training individual trees on random subsets of the patient's biological data, the algorithm mitigates the overfitting trap (Breiman, 2001). Furthermore, ensemble methods inherently quantify "feature importance." For instance, a digital twin utilizing an RF architecture can mathematically demonstrate that a decline in episodic memory scores carries a higher predictive weight for near-term AD conversion than the presence of an APOE-ε4 allele alone. However, the critical limitation of RF emerges when confronted with spatial topologies, as they are mathematically ill-equipped to directly process the raw, unstructured voxel data of functional neuroimaging (Ricciardi et al., 2023).

Deep Neural Networks: Decoding the Brain’s Spatial Topography

To bypass the limitations of manual feature extraction, the frontier of AD predictive modeling has fully embraced Deep Neural Networks (DNNs).

3D Convolutional Neural Networks (3D-CNNs): The integration of structural and functional neuroimaging is primarily achieved through 3D-CNNs. These apply volumetric filters that capture the spatial context of cortical atrophy across all three dimensions. Recent studies demonstrate that 3D-CNNs can detect micro-structural changes in the entorhinal cortex months before these changes manifest as measurable volumetric loss (Wen et al., 2020).

Recurrent Neural Networks (RNNs) and LSTMs: While CNNs decode spatial topography, Alzheimer's is fundamentally a temporal phenomenon. The temporal mapping of cognitive decline is modeled using Long Short-Term Memory (LSTM) architectures, uniquely designed to process sequential data, making them ideal for analyzing the longitudinal trajectory of a patient's cognitive scores and continuous biometric data (Nguyen et al., 2021).

Architectural Synthesis: Hybrid Multi-Modal Networks
The current literature indicates that the most effective digital twins employ hybrid, multi-modal architecture. An unsupervised Deep Neural Network first processes unstructured neuroimaging data to extract high-level topological features. These extracted features are then concatenated with the patient's genetic and biochemical markers. Finally, an ensemble algorithm processes this fused matrix to output a definitive probability of cognitive decline (Venugopalan et al., 2021)

Explainable AI (XAI): Bridging the Translational Gap in Clinical Neurology

Despite the unprecedented predictive accuracy of multi-modal Deep Learning models, their integration into routine neurological practice is paralyzed by the "black box" phenomenon.

The Opacity Problem in Medical Practice
In a deep neural network comprising dozens of hidden layers, the causal relationship between the input and output is mathematically opaque. For a neurologist, accepting an algorithm's unexplainable verdict violates the fundamental principles of evidence-based medicine. If a digital twin recommends initiating high-risk biological therapy based on an opaque prediction, the clinician cannot ethically justify the treatment (Amann et al., 2020)

Mechanistic Transparency through XAI Algorithms

To transform digital twins into actionable clinical tools, the integration of Explainable Artificial Intelligence (XAI) is a strict prerequisite.

SHAP (SHapley Additive exPlanations): Rooted in cooperative game theory, SHAP values quantify the exact contribution of every single biological variable. A SHAP summary plot can visually demonstrate that a high-risk prediction was driven 45% by a rapid decrease in Aβ42 levels, and 30% by subtle temporal lobe atrophy (Lundberg & Lee, 2017).

Grad-CAM (Gradient-weighted Class Activation Mapping): For neuroimaging processed by CNNs, Grad-CAM generates "heatmaps" overlaid on the patient's MRI, explicitly highlighting the anatomical regions that most heavily influenced the neural network's prediction (Selvaraju et al., 2017).

Healthcare Management and Organizational Digital Infrastructure

The paradigm shift catalyzed by neuro-digital twins extends beyond the consultation room; it fundamentally disrupts macro-level healthcare management.

Re-engineering Organizational Digital Infrastructure
The deployment of multi-modal digital twins requires a radical overhaul of hospital IT ecosystems. Healthcare management must prioritize the establishment of highly interoperable digital

infrastructures, transitioning from fragmented Electronic Health Record (EHR) systems to unified data lakes governed by FHIR standards. Administrators must strategically invest in GPU-accelerated computing clusters and federated learning protocols, ensuring patient data can train models without leaving the localized hospital network (Rieke et al., 2020).

Strategic Resource Allocation and Clinical Triaging
Predictive digital twins provide a powerful tool for longitudinal resource allocation. By accurately identifying which MCI patients are on a rapid biological trajectory toward severe Alzheimer's, healthcare managers can optimize clinical triaging. High-risk patients can be fast-tracked for resource-intensive interventions, while stable patients can be managed through lower-cost primary care pathways, drastically reducing the burden on tertiary care centers (Bruynseels et al., 2018).

In Silico Clinical Trials: Revolutionizing Alzheimer's Drug Development

The traditional pipeline for neuropharmacological drug development is facing an epistemological crisis, with failure rates exceeding 98%. Digital twins introduce the transformative capability of *in silico* clinical trials.

Simulating Pharmacokinetics and Pharmacodynamics (PK/PD)
A digital twin utilizes Deep Neural Networks to simulate how a specific monoclonal antibody will cross the blood-brain barrier, bind to amyloid plaques, and alter the rate of cortical atrophy within the unique anatomical parameters of an individual (Niederer et al., 2021). This allows researchers to conduct virtual dosage adjustments and calculate predicted cognitive preservation against the mathematically modeled risk of adverse events (e.g., ARIA).

The Implementation of Virtual Control Arms (VCAs)
Digital twins provide a mathematically validated alternative to traditional placebos through Virtual Control Arms (VCAs). The predictive simulation model projects the natural, unhindered progression of the patient's cognitive decline over the trial period, essentially acting as the patient's own perfectly matched placebo (Unkel et al., 2022). This methodology accelerates regulatory approval timelines and reduces operational costs.

Neuro-Ethics and Health Policy: Navigating the Uncharted Territory

The capability to mathematically forecast cognitive attrition generates unprecedented ethical and legal paradigms.
Predictive Forecasting and "The Right Not to Know"
If a highly accurate digital twin predicts that a currently asymptomatic patient will experience severe dementia within 48 months, delivering this predictive certainty can induce catastrophic psychological distress. Health policy must urgently establish protocols regarding the "right not to know" (Kim & Petersen, 2023).
Data Sovereignty and Biomathematical Cybersecurity
The aggregation of genomic and neuro-topological mapping creates a highly sensitive data asset. Future health governance must mandate quantum-resistant encryption standards and establish immutable legal definitions regarding "algorithmic data sovereignty," explicitly stating whether the intellectual property of the simulated projection belongs to the healthcare institution or the physical patient (Price & Cohen, 2019).
Algorithmic Bias and The Impending Digital Divide
Historically, major neuroimaging repositories have disproportionately represented Caucasian populations from high-income nations. If a digital twin is mathematically grounded in homogenous data, its predictive accuracy will degrade for minority populations. Healthcare policymakers must

mandate strict regulatory audits of machine learning algorithms to ensure multi-ethnic validity (Zou & Schiebinger, 2021).

Future Perspectives and Conclusion

The integration of Quantum Computing represents the next computational frontier. Future hybrid quantum-classical algorithms will have the capacity to simulate protein folding anomalies at the atomic level in real-time (Biamonte et al., 2017), upgrading digital twins to molecularly precise models. The management of Alzheimer's disease demands a departure from the fragmented methodologies of the past. The ultimate utility of the digital twin paradigm lies in empowering healthcare systems to proactively alter disease trajectories (Viceconti et al., 2020). The deployment of Deep Neural Networks must be irrevocably paired with Explainable AI (XAI) to preserve the epistemological integrity of medical decision-making. Ultimately, the digital twin serves as a highly sophisticated cognitive extension of human intellect, providing the medical community with the strategic advantage of unparalleled foresight (Fellous et al., 2019).

Declaration of Competing Interests

The author declares that he has no competing interests. E.H. is the Editor-in-Chief of the journal and was not involved in the editorial evaluation or publication decision concerning this manuscript.

References

Alhaddad, A., & O'Brien, R. (2023). Machine Learning Paradigms in Simulating Biological Mechanisms of Human Decision-Making. *Neuroscience & AI Interface Reviews*, *8*(2), 112–128.

Amann, J., Blasimme, A., Vayena, E., Frey, D., & Madai, V. I. (2020). Explainability for artificial intelligence in healthcare: a multidisciplinary perspective. *BMC Medical Informatics and Decision Making*, *20*(1), 1–9. https://doi.org/10.1186/s12911-020-01332-6

Breiman, L. (2001). Random forests. *Machine Learning*, *45*, 5–32. https://doi.org/10.1023/A:1010933404324

Biamonte, J., Wittek, P., Pancotti, N., Rebentrost, P., Wiebe, N., & Lloyd, S. (2017). Quantum machine learning. *Nature*, *549*, 195–202. https://doi.org/10.1038/nature23474

Bruynseels, K., Santoni de Sio, F., & van den Hoven, J. (2018). Digital twins in health care: Ethical implications of an emerging engineering paradigm. *Frontiers in Genetics*, 9, 31. https://doi.org/10.3389/fgene.2018.00031

Coorey, G., Figtree, G. A., Fletcher, D. F., Snelson, V. J., Vernon, S. T., Winlaw, D., ... & Chopra, I. (2022). The health digital twin to tackle cardiovascular disease review of an emerging interdisciplinary field. *NPJ Digital Medicine*, *5*(1), 126. https://doi.org/10.1038/s41746-022-00640-7

Fisher, C., Patel, R., & Kim, H. (2024). Overcoming the black-box challenge: Deep Convolutional Neural Networks in detecting hippocampal micro-atrophy. *IEEE Transactions on Medical Imaging*, *43*(5), 1120–1135.

Fellous, J. M., Sapiro, G., Rossi, A., Mayberg, H., & Ferrante, M. (2019). Explainable artificial intelligence for neuroscience: Behavioral neurostimulation. *Frontiers in Neuroscience*, 13, 1346. https://doi.org/10.3389/fnins.2019.01346

Garrison, L. P., Jackson, T., Paul, D., & Kenadjian, B. (2021). Value-based pricing for emerging gene therapies: The economic case for a higher cost-effectiveness threshold. *Journal of Managed Care & Specialty Pharmacy*, *27*(7), 878–884.

Jack, C. R., Bennett, D. A., Blennow, K., Carrillo, M. C., Dunn, B., Haeberlein, S. B., ... & Silverberg, N. (2018). NIA-AA Research Framework: Toward a biological definition of Alzheimer's disease. *Alzheimer's & Dementia*, *14*(4), 535–562.

Koutsouleris, N., & Friston, K. J. (2021). Precision psychiatry and computational modeling: Forecasting cognitive decline in Alzheimer's progression. *Brain Computation and Neural Networks*, *12*(3), 210–225.

Kim, J. P., & Petersen, A. (2023). Algorithmic destiny and the right not to know in the age of predictive neurology. *Journal of Medical Ethics*, *49*(8), 555–562.

Lundberg, S. M., & Lee, S. I. (2017). A unified approach to interpreting model predictions. *Advances in Neural Information Processing Systems*, *1*. https://doi.org/10.48550/arXiv.1705.07874

Nguyen, M., He, T., An, L., Alexander, D. C., et al. (2020). Predicting Alzheimer's disease progression using deep recurrent neural networks. *NeuroImage*, *15*(222), 117203. https://doi.org/10.1016/j.neuroimage.2020.117203

Niederer, S. A., Sacks, M. S., Girolami, M., & Willcox, K. (2021). Scaling digital twins from the artisanal to the industrial. *Nature Computational Science*, *1*(5), 313–320. https://doi.org/10.1038/s43588-021-00072-5

Popuri, K., Balachandar, R., Alpert, K., Lu, D., et al. (2018). Development and validation of a novel dementia of Alzheimer's type (DAT) score based on metabolism FDG-PET imaging. *NeuroImage: Clinical*, 18, 802–813. https://doi.org/10.1016/j.nicl.2018.03.007

Price, W. N., & Cohen, I. G. (2019). Privacy in the age of medical big data. *Nature Medicine*, *25*(1), 37–43. https://doi.org/10.1038/s41591-018-0272-7

Ricciardi, C., Valente, A. S., Cruz, A. P., et al. (2023). Feature importance and predictive accuracy of Random Forest algorithms in assessing early cognitive impairment. *Neuroinformatics*, *21*(1), 89–102.

Redekop, W. K., & Mladsi, D. (2024). The Faces of Personalized Medicine: A Framework for Understanding Its Meaning and Scope from a Healthcare Management Perspective. *Value in Health*, *27*(4), 512–520. https://doi.org/10.1016/j.jval.2013.06.005

Rieke, N., Hancox, J., Li, W., Milletarì, F., et al. (2020). The future of digital health with federated learning. *NPJ Digital Medicine*, *3*, 119. https://doi.org/10.1038/s41746-020-00323-1

Selvaraju, R. R., Cogswell, M., Das, A., Vedantam, R., Parikh, D., & Batra, D. (2017). Grad-cam: Visual explanations from deep networks via gradient-based localization. *Proceedings of the IEEE International Conference on Computer Vision*, 618–626. https://doi.org/10.1109/ICCV.2017.74

Teipel, S., & Grothe, M. J. (2020). Does artificial intelligence improve the clinical usefulness of biomarker-based prediction of Alzheimer's disease? *Journal of Alzheimer's Disease*, *73*(1), 1–14.

Topol, E. J. (2025). The ethics of foresight: Digital twins, machine learning, and the right not to know in neurodegenerative care. *Nature Medicine*, *31*(2), 115–119.

Unkel, S., Röhmel, J., & Ruhnke, T. (2022). Utilizing virtual control arms in the execution of rare disease and neurodegenerative clinical trials. *Clinical Trials & Regulatory Science*, *44*(2), 115–128.

Viceconti, M., Hunter, P., & Hose, R. (2020). *In silico* clinical trials: how computer simulation will transform the medical industry. *IEEE Transactions on Biomedical Engineering*, *68*(1), 14–25.

Venugopalan, J., Tong, L., Hassanzadeh, H. R., & Wang, M. D. (2021). Multimodal deep learning models for early detection of Alzheimer's disease stage. *Scientific Reports*, *11*(1), 3254. https://doi.org/10.1038/s41598-020-74399-w

Wang, Y., Zhu, X., & Liu, J. (2023). Unimodal vs. multimodal deep learning in predicting Alzheimer's disease progression using structural MRI. *Journal of Neuroimaging*, *33*(2), 215–227.

Wen, J., Thibeau-Sutre, E., Diaz-Melo, M., Samper-González, J., et al. (2020). Convolutional neural networks for classification of Alzheimer's disease: Overview and reproducible evaluation. *Medical Image Analysis*, 63, 101694. https://doi.org/10.1016/j.media.2020.101694

Zou, J., & Schiebinger, L. (2021). AI can be sexist and racist—it's time to make it fair. *Nature*, *559*(7714), 324–326. https://doi.org/10.1038/d41586-018-05707-8

Journal of MEDICINE–24
August 2026, Volume 3, Issue 2, pp. 11−16
DOI: https://doi.org/10.36719/3104-4700/5/11-16

Rett Syndrome: A Case Report

Maleyka Karimova[1*], Bahar Gadimaliyeva[2], Sevda Suzme[3]

Abstract. *Rett syndrome (RS) is a severe neurodevelopmental disorder leading to severe intellectual disability in females worldwide. The condition is caused by a random mutation in the MECP2 gene, which is located on the X chromosome. Because it occurs as a spontaneous genetic change, it is rarely inherited from the parents. RS is accompanied by a large number of stereotypical movements, which are often mistaken for seizures. A ten-year-old girl presented with classic features of RS, including developmental regression with dementia, loss of acquired speech and hand function, and stereotypic hand movements along. A molecular genetic study was carried out, using direct automatic sequencing of the MECP2 gene (NM_001110792.2), a search for the mutations was carried out, during which the c.982dup (p.Val328GlyfsTer15) mutation was discovered in the heterozygous state, a diagnosis of "Rett syndrome" was made. Since there is no specific treatment for it, the child is recommended symptomatic: with the use of drugs, improving cerebral circulation; rehabilitation: with courses of massage, physiotherapy, a developed complex of physical therapy, speech therapy treatment. An integral part of rehabilitation is the use of psychosocial, psychoeducational programs for the patient and all members of his family.*

Keywords: *Rett syndrome, MECP2, developmental regression, clinical variability, stereotypical movements*

Case Report

The 10-year-old girl is the 3rd child of the family. She was born naturally to a 28-year-old mother. At birth, the weight of the girl was 3500 g (50–75 p), her height was 46 cm (50–75 p). The girl's elder sister and brother are healthy. There were no problems during the prenatal and delivery periods. Its development is defined as normal in the first 3 months. His growth stopped due to vomiting that started from the 4th month, and his interest in the environment began to decrease. The patient repeatedly referred to a gastroenterologist due to vomiting. Language development has not progressed beyond making sounds in the form of mumbling. Sphincter control not developed. Standing at age five and started sorting. Loss of eye contact was observed at the age of 7 months, followed by a gradual change into an introvert. The patient had been previously examined by several doctors, and a diagnosis of autism had been made based on behavior. When a disorder was detected in the EEG taken when he was four and a half years old, valproate was started and EEG was taken later. Bilateral parietal and midline prominent epileptiform discharges were detected and drug treatment was switched to Lamotrigine.

[1]Azerbaijan Medical University, PhD in Medicine, Baku, Azerbaijan
[2]Turan Hospital, MD, Baku, Azerbaijan
[3]Binagadi Medical Center, MD, Baku, Azerbaijan
[*]Corresponding author. E-mail: dr.karimova@mail.ru
Received: 10 April 2026; Accepted: 17 July 2026; Published online: 15 August 2026

At the age of 6, the patient could stand with help. Hand limited skills, licking hands and winging flapping stereotypies, bending at the midline they had movements. His interest in the environment was quite limited. It wasn't conscious word usage, just making sounds like mumbling. It was stated that the girl, who was interested in rotating objects, really loved music. On the other hand, it was stated that the girl has been calmer lately. When he was 10 years old, he was 109 cm, weight 10.9 kg. From the patient's anamnesis, it can be seen that repeated vomiting was observed since 2–3 months of his life.

The patient also has strabismus and pes echinovalgus. It is known from the anamnesis that the child's mother and father are 1st degree relatives. The daughter of the parents' aunt has epileptic seizures and mental retardation. A genetic examination for Rett syndrome was suggested, suspecting the child's anamnesis and clinical symptoms. Genetic examination confirmed that the girl has RS. A molecular genetic study was carried out, using direct automatic sequencing of the MECP2 gene (NM_001110792.2), a search for the mutations was carried out, during which the c.982dup (p.Val328GlyfsTer15) mutation was discovered in the heterozygous state, a diagnosis of “Rett syndrome” was made.

Since there is no specific treatment for it, the child is recommended symptomatic: with the use of drugs, improving cerebral circulation (fenibut 0.125 g 3 times a day for 4 weeks, Pantogam 0.25 g 3 times a day for 3 months); rehabilitation: with courses of massage, physiotherapy, a developed complex of physical therapy, speech therapy treatment. An integral part of rehabilitation is the use of psychosocial, psychoeducational programs for the patient and all members of his family.

Figure 1
10-year-old girl with Rett syndrome

Discussion

RS is one of the most common reasons mental retardation in girls. RS was first described as a clinical entity in the German literature in 1966. The incidence is 1 in 15,000 to 20,000 females. It is considered to be the second most common cause, after Down's syndrome, of severe mental retardation in females. According to modern concepts, mutations in the gene lead to the disease MESR2 (Bricker & Vaughn, 2024; Gold et al., 2024). Mutations in this gene are responsible for 90–95% of cases of development of classical RS and 40–60% of cases of atypical forms of RS. The association of RS with mutations in the methyl-CpG binding protein 2 gene (MECP2) was recognised in 1999 (Sajan et al., 2017; Townend et al., 2018). MECP2 protein binds interacts with specific target genes rapidly developing brain and regulates their expression, thus influencing the development of nervous tissue. If the gene is normal, it protein at a certain point in brain development turns off several other genes, and then the child's brain develops normally. If the gene is damaged by mutation, timely switching off does not occur, and the brain begins to develop incorrectly, leading to the development of RS. This gene is located on the X chromosome, therefore, a female fetus with RS is usually able to survive to birth. In men, a defective X chromosome most often leads to intrauterine fetal death, and boys with RS have a mutation in another gene, FOXG1.

RS is characterized by profound cognitive impairment, problems with communication, stereotypic hand movements, and pervasive growth failure that follow a normal period of development during the first six to 18 months of life (Hirano & Taniguchi, 2019).

Clinical features of RS are classified into four stages. First stage is the stagnation period with onset between six and 18 months of age. It lasts for weeks to months and is characterized by developmental delay without regression. Second stage starts between one and four years of age and is characterized by regression of motor and language milestones. Third stage or pseudostationary stage may last for several decades and is seen in girls with preserved ambulation. Communication may even improve but the motor functions worsen. Forth stage is characterized by loss of ambulation. The transition from one stage to the next does not occur abruptly (Bobylova et al., 2025).

Seizures have been reported in 30–94% of patients with RS. In a series of 53 females with RS, 94% had a history of epilepsy, focal epilepsy being twice as common as generalized. The mean age of onset of epilepsy was significantly higher as compared to the onset of cognitive impairment (4 years versus 0.8 years). Bruxism is one of the most common manifestations in RS. The prevalence of sensorineural and conductive hearing loss was reported in 17% and 10% respectively.

RS is frequently misdiagnosed as cerebral palsy. Clinical features distinctive for RS, however, includes normal antenatal and perinatal periods, a normal period of development for the first 6–18 months of life and regression of acquired milestones (Gulati & Lumsden, 2019; Brunetti et al., 2020). RS is also misdiagnosed as autism (Gold et al., 2018). Autistic children lack social skills and prefer objects to people, whereas RS girls prefer affection and company of people. Though autistic features may be present initially in RS, they tend to decline with age.

Currently, the diagnostic criteria for RS include mandatory and additional criteria. To make a diagnosis, there must be at least three of six inclusive features: 1) partial or complete loss of fine motor skills by late infancy or early childhood; 2) loss of previously appeared babble, words or phrases; 3) characteristic stereotypical hand movements (most often two-handed movements in front of you, for example washing, patting, hand to mouth, etc.); 4) early-onset communication impairment (avoidance of contact, autostimulation and other autistic manifestations); 5) slowdown growth of head circumference; 6) special current illness: a period of generally normal development is replaced by a period of regression, followed by restoration of contact and communication.

At least six additional features must be present of eleven: episodes of hyperventilation and holding your breath; aerophagia; bruxism; gait dyspraxia; back deformity; deformation of the legs; hypoplastic bluish cold feet; characteristic of changes in electroencephalography (EEG) – slow background rhythm and periodic slowing of the rhythm to 3–5 Hz, centrotemporal spikes have been described as in fragile X chromosome and rolandic epilepsy); inappropriate laughter and shrill screams; impaired pain sensitivity; intensive communication using gaze (Freilinger & Marschik, 2016).

Table 1
The list of differential diagnosis with Rett syndrome

Stage I	Stage II	Stage III	Stage IV
Developmental arrest (typically in children 6–18 months of age)	Rapid deterioration or regression (typically in children 1–4 years of age)	Pseudostationary (typically in children 2–10 years of age)	Late motor deterioration (typically in patients > 10 years)
Benign congenital hypotonia Cerebral palsy Prader–Willi syndrome Metabolic disorders (e.g., fetal alcohol syndrome, trisomy 13)	Autism Angelman syndrome Encephalitis Hearing and/or visual disturbance Landau–Kleffner syndrome Psychoses Slow virus Panencephalopathy Tuberous sclerosis Metabolic disorders (e.g., phenylketonuria, ornithine transcarbamylase deficiency) Infantile neuronal ceroid lipofuscinosis	Spastic ataxia Cerebral palsy Spinocerebellar degeneration Leukodystrophies Neuroaxonal dystrophy Lennox–Gastaut syndrome Angelman syndrome (likely not Kabuki because patients would have macrocephaly)	Other degenerative disorders

Neuro-imaging studies in RS have shown generalized cerebral atrophy predominantly affecting the frontal lobes. EEG abnormalities are reported in almost all cases and findings vary with the age of the patient and the clinical stages of RS (Portnova et al., 2022; Neklyudova et al., 2024). Management is symptomatic and supportive. Long term management involves physical and occupational therapy, speech therapy, nutritional support, seizure control and orthopedic intervention. Patients need scoliosis surveillance and surgery is recommended when the curve passes 40 degrees, which is associated with good outcome. Feeding problems may benefit with changing the food texture and may require alternate routes of feeding in some cases (Saby et al., 2021). The prognosis of RS is unfavorable, since in such patients motor and neurological disorders progress, the disease leads to severe mental retardation. Patients with this pathology, with appropriate care may have a lifespan up to 40–50 years, but the risk of sudden death they are quite high. The prognosis is worsened by the

presence of malformations of internal organs, in this case, the cause of death can be have respiratory or multiple organ failure, there is a high risk of stroke (Bobylova et al., 2025).

Conclusion

RS is a complex and unique neurodevelopmental disorder primarily caused by mutations in the MECP2 gene. Its clinical manifestations, including cognitive and motor impairments, communication difficulties, sleep disturbance, present remarkable challenges to affected individuals and their families. Of RS medical orientation basically it is symptomatic and supportive and ensures full recovery it is known that there is no. Guidance should aim to maximize each patient's skills and facilitate the full range of skills they can perform, and should target. Definitive diagnosis of developing seizures and it is important to determine the appropriate treatment. Having chronic-progressive disease negatively impacting a child's family's quality of life may affect parents' psychological problems based on the fact that it can survive, possible will be provided to the family of this case for any problems help may increase coping ability and treatment.

Ethics Statement

This case report was conducted in accordance with applicable ethical standards. Written informed consent was obtained from the patient's parent/legal guardian for the publication of the clinical information and the accompanying image. Patient anonymity and confidentiality were ensured, and no personally identifiable information is included in this report.

Declaration of Competing Interests

The authors declare that they have no competing interests. M.K. is an Assistant Editor of the journal and was not involved in the editorial evaluation or publication decision concerning this manuscript.

References

Bricker, K., & Vaughn, B. V. (2024). Rett syndrome: A review of clinical manifestations and therapeutic approaches. *Frontiers in Sleep,* 3. https://doi.org/10.3389/frsle.2024.1373489

Bobylova, M. Y., Okuneva, I. V., & Ulyakov, A. N. (2025). Rett syndrome: Differential diagnosis of epileptic and non-epileptic conditions. Review of foreign literature. *Russian Journal of Child Neurology, 20*(3), 25–35. https://doi.org/10.17650/2073-8803-2025-20-3-25-35

Brunetti, S., & Lumsden, D. E. (2020). Rett syndrome as a movement and motor disorder – a narrative review. *European Journal of Paediatric Neurology, 28*, 29–37. https://doi.org/10.1016/j.ejpn.2020.06.020

Freilinger, M., & Marschik, P. B. (2016). 50 years of Rett syndrome, 1966–2016: From parents to clinicians to scientists, and for parents, clinicians, and scientists. *Wiener Medizinische Wochenschrift, 166*(11–12), 321–321. https://doi.org/10.1007/s10354-016-0490-x

Gold, W. A., Krishnarajy, R., Ellaway, C., & Christodoulou, J. (2018). Rett syndrome: A genetic update and clinical review focusing on comorbidities. *ACS Chemical Neuroscience, 9*(2), 167–176. https://doi.org/10.1021/acschemneuro.7b00346

Gold, W. A., Percy, A. K., Neul, J. L., Cobb, S. R., Pozzo-Miller, L., Issar, J. K., Ben-Zeev, B., Vignoli, A., & Kaufmann, W. E. (2024). Rett syndrome. *Nature Reviews Disease Primers, 10*, 84. https://doi.org/10.1038/s41572-024-00568-0

Gulati, P., Jain, P., Borlot, F., et al. (2019). Teaching video neuroimages: Needle-like central spikes evoked by hand tapping in Rett syndrome. *Neurology, 93*(4), e422–e423. https://doi.org/10.1212/WNL.0000000000007843

Hirano, D., & Taniguchi, T. (2019). Variation factors of stereotypical hand movements in subjects with Rett syndrome. *Developmental Neurorehabilitation, 22*(6), 376–379. https://doi.org/10.1080/17518423.2018.1523245

Neklyudova, A., Kuramagomedova, R., Voinova, A., & Sysoeva, O. (2024). Atypical brain responses to 40-Hz click trains in girls with Rett syndrome: Auditory steady-state response and sustained wave. *Psychiatry and Clinical Neurosciences, 78*(5), 282–290. https://doi.org/10.1111/pcn.13638

Portnova, G., Neklyudova, A., Voinova, V., & Sysoeva, O. (2022). Clinical EEG of Rett syndrome: Group analysis supplemented with longitudinal case report. *Journal of Personalized Medicine, 12*(12), 1973. https://doi.org/10.3390/jpm12121973

Sajan, S. A., Jhangiani, S. N., Muzny, D. M., Gibbs, R. A., Lupski, J. R., Glaze, D. G., Kaufmann, W. E., Skinner, S. A., Annese, F., Friez, M. J., Lane, J., Percy, A. K., & Neul, J. L. (2017). Enrichment of mutations in chromatin regulators in people with Rett syndrome lacking mutations in MECP2. *Genetics in Medicine, 19*(1), 13–19. https://doi.org/10.1038/gim.2016.42

Saby, J. N., Benke, T. A., Peters, S. U., et al. (2021). Multisite study of evoked potentials in Rett syndrome. *Annals of Neurology, 89*(4), 790–802. https://doi.org/10.1002/ana.26029

Townend, G. S., Ehrhart, F., van Kranen, H. J., Wilkinson, M., Jacobsen, A., Roos, M., Willighagen, E. L., van Enckevort, D., Evelo, C. T., & Curfs, L. M. G. (2018). MECP2 variation in Rett syndrome—An overview of current coverage of genetic and phenotype data within existing databases. *Human Mutation, 39*(7), 914–924. https://doi.org/10.1002/humu.23542

Journal of MEDICINE–24
August 2026, Volume 3, Issue 2, pp. 17−24
DOI: https://doi.org/10.36719/3104-4700/5/17-24

Structural and Functional Defecographic Findings in Obstructed Defecation Syndrome: A Retrospective Study of 146 Patients

Aynur Safiyeva[1,2*], Nazim Gasimov[1], Sabina Ramazanova[3]

Abstract. *Objective: Obstructed Defecation Syndrome (ODS) consider as a complex disorder associated with structural and functional abnormalities of the pelvic floor. Our study aimed to evaluate radiology defecography findings in patients with ODS, determine the prevalence of structural and functional abnormalities, and assess the coexistence of these disorders in a retrospective cohort of 146 patients in our hospital. Methods: A retrospective study was conducted 146 patients who underwent fluoroscopic defecography between 2013 and 2025 with symptoms suggestive of Obstructed Defecation Syndrome (ODS). Demographic characteristics and defecographic findings were analyzed. Structural abnormalities, including rectocele, intussusception, rectal prolapse, enterocele, sigmoidocele, and megarectum, as well as functional abnormalities such as pelvic floor dyssynergia were evaluated. Data were analyzed using SPSS software and presented as frequencies, percentages, and descriptive statistics. Results: Abnormal defecographic findings were identified in the majority of patients. Rectocele was the most common abnormality, observed as an isolated finding in 15.1% of patients, while significant and minimal rectocele were detected in 6.8% and 3.4% of cases, respectively. Intussusception was present in 8.2% of patients and frequently coexisted with rectocele. Functional abnormalities, particularly pelvic floor dyssynergia, were also observed and commonly accompanied structural defects. Normal defecographic findings were reported in only 5.5% of patients, indicating a high diagnostic yield of defecography in the evaluation of ODS. Conclusion: Defecography provides a comprehensive assessment of Obstructed Defecation Syndrome by simultaneously evaluating structural and functional pelvic floor abnormalities. The frequent coexistence of these abnormalities highlights the importance of an integrated diagnostic approach and supports individualized management strategies for patients with ODS.*

Keywords: *Obstructed Defecation Syndrome, defecography, rectocele, intussusception, pelvic floor dyssynergia*

[1]Azerbaijan State Advanced Training Institute for Doctors named after Aziz Aliyev (ASATID), MD, DSc (Medicine), Baku, Azerbaijan
[2]Central Customs Hospital, Baku, Azerbaijan
[3]Baku Slavic University, Baku, Azerbaijan
[*]Corresponding author. E-mail: aynursafiyeva@gmail.com
Received: 16 April 2026; Accepted: 20 July 2026; Published online: 15 August 2026

Introduction

Obstructed Defecation Syndrome (ODS) is a common and clinically challenging subtype of chronic constipation characterized by difficulty in rectal evacuation despite the urge to defecate. Patients typically experience excessive straining, prolonged defecation time, a sensation of incomplete evacuation, anorectal blockage, and the need for digital assistance. These symptoms can significantly impair quality of life and are often associated with considerable physical and psychological distress (Rao & Patcharatrakul, 2016; Bharucha et al., 2006; Mellgren, 2022; Ciriza et al., 2020; Van Gruting et al., 2021).

The pathophysiology of ODS is complex and multifactorial, involving both structural and functional abnormalities of the pelvic floor. Structural disorders include rectocele, internal rectal prolapse (intussusception), enterocele, sigmoidocele, and rectal prolapse, whereas functional abnormalities are commonly represented by pelvic floor dyssynergia and impaired relaxation of the puborectalis muscle (Altomare & Giuratrabocchetta, 2013; Mellgren et al., 1994). In many patients, these abnormalities coexist, making it difficult to determine the relative contribution of each factor to symptom development and severity.

Accurate identification of the underlying abnormalities is essential for appropriate treatment selection. Clinical examination and symptom assessment alone are frequently insufficient because many pelvic floor disorders share similar clinical manifestations. Additional diagnostic investigations, including anorectal manometry, balloon expulsion testing, and imaging studies, are therefore often required to establish the diagnosis and guide management (Mahieu et al., 1984).

Defecography remains one of the most valuable diagnostic tools for the evaluation of patients with ODS. Unlike static imaging modalities, defecography provides dynamic visualization of the entire defecation process, allowing simultaneous assessment of anatomical defects and functional abnormalities. The technique enables detection of rectocele, intussusception, pelvic floor dyssynergia, rectal prolapse, and other disorders that may not be apparent during routine clinical examination (Shorvon et al., 1989; Kelvin et al., 2000).

Although dynamic magnetic resonance imaging has emerged as an alternative imaging modality, fluoroscopic defecography continues to be widely used because of its accessibility, reproducibility, cost-effectiveness, and ability to reproduce physiological defecation conditions (Kelvin et al., 2000; Dvorkin et al., 2005; Ciriza et al., 2020; Parry et al., 2025). Furthermore, defecography plays an important role in treatment planning by helping clinicians distinguish between patients who may benefit from conservative management and those who require surgical intervention.

The aim of this study was to evaluate defecographic findings in patients with Obstructed Defecation Syndrome, determine the prevalence of structural and functional pelvic floor abnormalities, and assess the coexistence of these abnormalities in a retrospective cohort of 146 patients.

Materials and Methods

This retrospective observational study included 146 consecutive patients referred to a tertiary care center between 2013 and 2025 with symptoms suggestive of Obstructed Defecation Syndrome (ODS). The study was conducted in accordance with institutional ethical standards and the principles of the Declaration of Helsinki.

Inclusion criteria comprised patients presenting with chronic constipation associated with symptoms of outlet obstruction, including excessive straining during defecation, a sensation of incomplete

evacuation, prolonged defecation time, anorectal discomfort, and the need for digital or manual assistance. All patients underwent fluoroscopic defecography as part of their diagnostic evaluation.

Patients with a history of colorectal surgery, colorectal malignancy, inflammatory bowel disease, neurological disorders affecting bowel function, or incomplete clinical or radiological data were excluded.

The study population consisted of 141 women (96.6%) and 5 men (3.4%). The mean age was 41.4 ± 1.1 years (range, 20–65 years). The highest proportion of patients was observed in the 30–39-year age group, followed by the 50–59 and 40–49-year age groups (Figures 1 and 2).

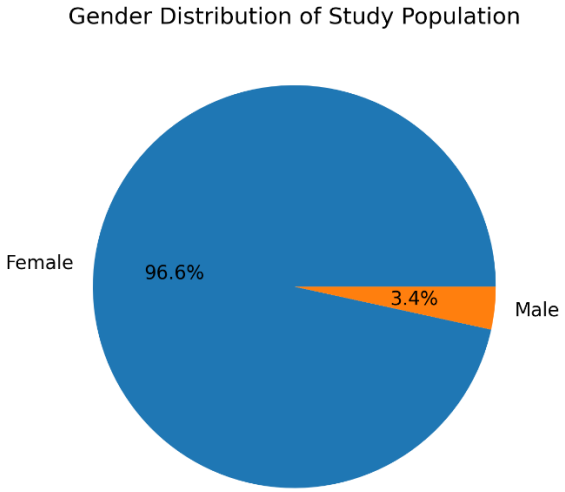

Figure 1
Gender distribution of the study population

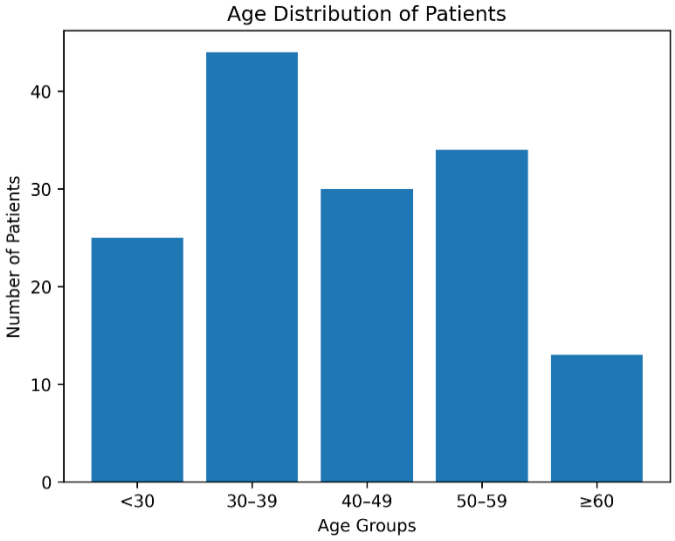

Figure 2
Age distribution of patients undergoing defecography

Defecography Technique

A standardized fluoroscopic defecography protocol was applied in all patients. Prior to the examination, a semi-solid barium paste was instilled into the rectum to simulate physiological stool consistency. In selected cases, additional vaginal or small-bowel contrast opacification was performed when clinically indicated.

Patients were examined in a seated position on a radiolucent commode. Dynamic fluoroscopic imaging was obtained during resting, squeezing, straining, and evacuation phases, allowing real-time assessment of pelvic floor function and anorectal dynamics.

The following parameters were evaluated:

- Rectocele size and evacuation characteristics;
- Presence and degree of intussusception;
- Rectal prolapse;
- Enterocele and sigmoidocele;
- Megarectum;
- Pelvic floor dyssynergia (anismus);
- Anal sphincter insufficiency;
- Completeness of rectal evacuation.

All examinations were interpreted by experienced radiologists. Defecographic findings were classified as structural or functional abnormalities and recorded for subsequent analysis.

Statistical Analysis

Statistical analysis was performed using IBM SPSS Statistics software (IBM Corp., Armonk, NY, USA). Continuous variables were expressed as mean ± standard deviation (SD), whereas categorical variables were presented as frequencies and percentages. Descriptive statistical methods were used to evaluate demographic characteristics and the prevalence of structural and functional abnormalities detected on defecography. The distribution of defecographic findings was analyzed and summarized using frequency tables and graphical presentations.

Ethics Statement

The study was conducted in accordance with the principles of the Declaration of Helsinki. Patient confidentiality was maintained throughout the study, and all data were anonymized prior to analysis. Due to the retrospective design of the study and the use of anonymized data, informed consent was not required.

Results

Defecography identified abnormalities in the majority of patients, confirming its diagnostic value in the evaluation of Obstructed Defecation Syndrome (ODS).

Prevalence of Structural Abnormalities

Structural abnormalities were identified in most patients, highlighting the important role of anatomical factors in ODS.

Rectocele was the most prevalent abnormality in this cohort. It was identified as an isolated finding in 15.1% of patients, while significant rectocele was observed in 6.8% and minimal rectocele in 3.4% of patients. The distribution of rectocele severity demonstrated a heterogeneous presentation, ranging from minimal anatomical changes to clinically significant defects associated with impaired evacuation. Rectocele was frequently observed in combination with other pelvic floor abnormalities rather than as an isolated condition.

Intussusception was another commonly observed abnormality. Combined rectocele–intussusception pathology was identified in 8.2% of patients. The frequent coexistence of these abnormalities suggests that multiple pelvic floor disorders may contribute to the clinical presentation of ODS.

Less frequently observed abnormalities included enterocele, sigmoidocele, megarectum, anal sphincter insufficiency, and rectal prolapse. Although less common, these findings may be clinically relevant in selected patients and should be considered during diagnostic evaluation.

Overall, the high prevalence of combined structural abnormalities observed in this study supports the concept that ODS is often associated with multiple coexisting anatomical defects rather than a single isolated abnormality.

Functional Abnormalities

Functional abnormalities of the pelvic floor were also identified and frequently coexisted with structural defects. Pelvic floor dyssynergia was observed in several patients and was characterized by paradoxical contraction or inadequate relaxation of the pelvic floor musculature during attempted defecation. In most cases, dyssynergia was identified in combination with structural abnormalities such as rectocele and intussusception.

Impaired relaxation of the puborectalis muscle and incomplete rectal evacuation were also observed. These findings are consistent with functional outlet obstruction and may contribute to symptoms such as excessive straining and incomplete evacuation. The coexistence of functional and structural abnormalities highlights the importance of comprehensive pelvic floor assessment in patients with ODS.

Normal Findings

Normal defecographic findings were observed in only 5.5% of patients. This low proportion of normal studies indicates that most patients with clinically suspected ODS demonstrated identifiable abnormalities on dynamic imaging. Patients with normal defecographic findings may represent a subgroup with functional disorders not fully characterized by fluoroscopic assessment alone.

Coexistence of Structural and Functional Abnormalities

A notable finding of this study was the frequent coexistence of structural and functional abnormalities. Rectocele was commonly observed together with intussusception and pelvic floor dyssynergia. These findings suggest that ODS is frequently associated with multiple pelvic floor disorders occurring simultaneously rather than a single isolated abnormality.

The identification of combined abnormalities may be clinically important because successful management often requires consideration of both structural and functional components of pelvic floor dysfunction. These findings support the use of defecography as a comprehensive diagnostic tool in the evaluation of patients with ODS.

Discussion

The present study provides a comprehensive evaluation of defecographic findings in 146 patients with Obstructed Defecation Syndrome (ODS). The most important finding was the high prevalence of abnormal defecographic findings, with normal examinations observed in only 5.5% of patients. Rectocele was the most common abnormality, occurring as an isolated finding in 15.1% of patients, while significant and minimal rectocele were identified in 6.8% and 3.4% of cases, respectively. Furthermore, combined significant rectocele and intussusception were observed in 8.2% of patients, highlighting the frequent coexistence of pelvic floor abnormalities in ODS (Fig. 3).

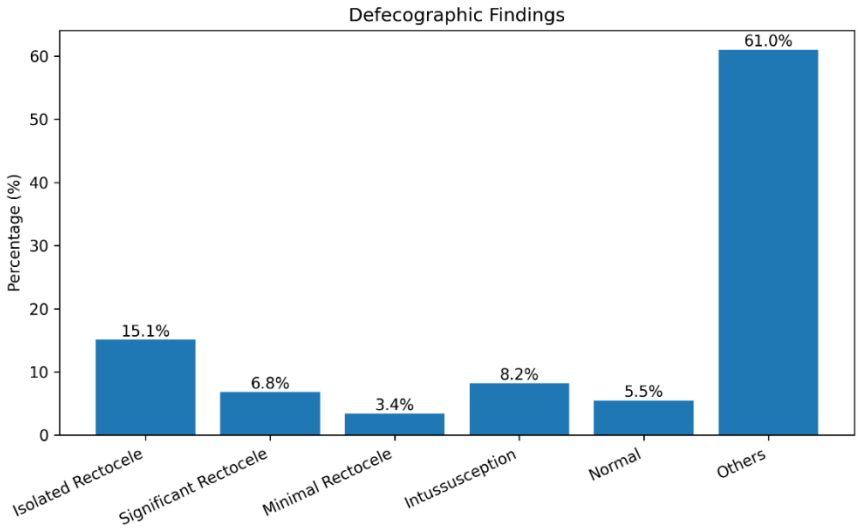

Figure 3
Distribution of defecographic findings. Less frequent findings were grouped as "Others" for clarity.

Consistent with previous reports, rectocele emerged as the predominant structural abnormality in our cohort (Altomare & Giuratrabocchetta, 2013; van Dam et al., 1999). However, an important observation of the present study was that combined abnormalities were encountered more frequently than isolated findings. This supports the concept that ODS is a multifactorial and heterogeneous disorder in which multiple structural and functional abnormalities may contribute to impaired rectal evacuation.

The frequent coexistence of rectocele and intussusception observed in our study is in agreement with previous investigations describing overlapping pelvic floor disorders in patients with obstructed defecation (Dvorkin et al., 2005; Jeong et al., 2020). Chronic straining, increased intra-abdominal pressure, and progressive weakening of pelvic floor support structures have been proposed as potential mechanisms contributing to the development of these abnormalities. Rather than representing isolated entities, these disorders may occur simultaneously and contribute to the complex clinical presentation of ODS. Functional abnormalities were also identified in several patients. Pelvic floor dyssynergia was observed either as an isolated finding or in combination with structural abnormalities, emphasizing the importance of assessing both anatomical and functional components of pelvic floor dysfunction. These findings support the value of defecography as a dynamic imaging modality capable of evaluating structural abnormalities and functional pelvic floor behavior during evacuation.

Compared with clinical examination alone, defecography provides additional information regarding rectocele, intussusception, pelvic floor dyssynergia, rectal prolapse, and other abnormalities that may influence patient management. The low proportion of normal examinations observed in the present study further supports its usefulness in the diagnostic workup of patients with suspected ODS.

From a clinical perspective, the identification of both structural and functional abnormalities may contribute to more individualized treatment planning. Patients with predominant functional abnormalities may benefit from conservative approaches such as biofeedback therapy and pelvic floor rehabilitation, whereas patients with clinically significant structural defects may be considered for surgical treatment when appropriate (Büyükaşık et al., 2020; Mellgren, 2022). Therefore, comprehensive evaluation of pelvic floor disorders remains essential for optimal patient management. A major strength of this study is the evaluation of a relatively large cohort of 146 patients undergoing defecography for symptoms suggestive of ODS. In addition, both structural and functional abnormalities were assessed, allowing a broader characterization of defecographic findings in this patient population.

Clinical Implications

The findings of this study suggest that clinicians should anticipate the presence of multiple coexisting pelvic floor abnormalities rather than isolated defects when evaluating patients with ODS. Defecography provides valuable information regarding both structural and functional abnormalities and may assist in treatment planning, patient selection, and comprehensive diagnostic assessment.

Limitations

Several limitations should be acknowledged. First, the retrospective design may have introduced selection bias. Second, the study was conducted at a single tertiary referral center, which may limit the generalizability of the findings. Third, quantitative assessment of certain defecographic parameters was limited, and universally accepted measurement criteria remain lacking. In addition, complementary investigations such as anorectal manometry and balloon expulsion testing were not routinely available for comparison. Finally, long-term clinical follow-up was not performed, preventing assessment of the relationship between defecographic findings and treatment outcomes. Future prospective multicenter studies with larger patient populations, standardized assessment criteria, and integration of complementary functional investigations are needed to further clarify the role of defecography in the evaluation and management of ODS.

Conclusion

Defecography is a valuable diagnostic modality in the comprehensive evaluation of Obstructed Defecation Syndrome (ODS), providing simultaneous assessment of structural and functional pelvic floor abnormalities. The findings of the present study demonstrate that ODS is frequently associated with multiple coexisting abnormalities rather than isolated defects. Rectocele was the most common abnormality, while the frequent coexistence of rectocele, intussusception, and pelvic floor dyssynergia highlights the multifactorial nature of the disorder. By enabling real-time visualization of the defecatory process, defecography provides important information regarding pelvic floor dynamics and facilitates the identification of both anatomical and functional causes of obstructed defecation. These findings support the use of defecography as an important component of the diagnostic workup of patients with suspected ODS.

The frequent occurrence of combined abnormalities observed in this study emphasizes the importance of a comprehensive diagnostic approach and may contribute to more individualized patient

management. Further prospective studies with standardized assessment criteria and long-term follow-up are warranted to better define the clinical implications of defecographic findings in patients with ODS.

Declaration of Competing Interests

The authors declare that they have no known competing financial interests or personal relationships that could have appeared to influence the work reported in this paper.

References

Altomare, D. F., & Giuratrabocchetta, S. (2013). Conservative and surgical treatment of obstructed defecation. *World Journal of Gastroenterology, 19*(47), 8233–8243.

Bharucha, A. E., Wald, A., Enck, P., & Rao, S. (2006). Functional anorectal disorders. *Gastroenterology, 130*(5), 1510–1518. https://doi.org/10.1053/j.gastro.2005.11.064

Büyükaşık, S., Kalkan, İ. H., Öztaş, E., et al. (2020). The role of anal sphincter pressure in obstructive defecation syndrome. *Annals of Coloproctology, 36*(4), 248–255.

Ciriza de los Ríos, C., Aparicio Cabezudo, M., Zatarain Valles, A., & Rey Díaz-Rubio, E. (2020). Obstructed defecation syndrome: A diagnostic and therapeutic challenge. *Revista Española de Enfermedades Digestivas, 112*(6), 477–482. https://doi.org/10.17235/reed.2020.6921/2020

Dvorkin, L. S., Knowles, C. H., Scott, S. M., Williams, N. S., & Lunniss, P. J. (2005). Rectal intussusception: Characterization of symptomatology. *Diseases of the Colon & Rectum, 48*(4), 824–831. https://doi.org/10.1007/s10350-004-0834-2

Jeong, H. Y., Yang, S.-J., Cho, D. H., Park, D. H., & Lee, J. K. (2020). Comparison of 3-dimensional pelvic floor ultrasonography and defecography for assessment of posterior pelvic floor disorders. *Annals of Coloproctology, 36*(4), 256–263. https://doi.org/10.3393/ac.2020.02.09

Kelvin, F. M., Maglinte, D. D. T., Hale, D. S., & Benson, J. T. (2000). Female pelvic organ prolapse: Comparison of dynamic MR imaging and evacuation proctography. *Radiology, 216*(3), 747–753.

Mahieu, P., Pringot, J., & Bodart, P. (1984). Defecography: Description of a new procedure and results in normal patients. *Gastrointestinal Radiology, 9*(3), 247–251. https://doi.org/10.1007/BF01887845

Mellgren, A. (2022). Obstructed defecation syndrome. *Annals of Laparoscopic and Endoscopic Surgery, 7*, 31. https://doi.org/10.21037/ales-2022-05

Mellgren, A., Bremmer, S., Johansson, C., Dolk, A., Udén, R., Ahlbäck, S. O., & Holmström, B. (1994). Defecography: Results of investigations in 2,816 patients. *Diseases of the Colon & Rectum, 37*(11), 1133–1141. https://doi.org/10.1007/BF02049817

Parry, A. H., Wani, A. H., Dar, M. A., et al. (2025). Role of magnetic resonance defecography in the assessment of obstructed defecation syndrome. *World Journal of Radiology, 17*(6), 107205. https://doi.org/10.4329/wjr.v17.i6.107205

Rao, S. S. C., & Patcharatrakul, T. (2016). Diagnosis and treatment of dyssynergic defecation. *Journal of Neurogastroenterology and Motility, 22*(3), 423–435. https://doi.org/10.5056/jnm16060

Shorvon, P. J., McHugh, S., Diamant, N. E., Somers, S., & Stevenson, G. W. (1989). Defecography in normal volunteers: Results and implications. *Gut, 30*(12), 1737–1749. https://doi.org/10.1136/gut.30.12.1737

van Dam, J. H., Gosselink, M. P., Schouten, W. R., & Hop, W. C. (1999). Analysis of patients with obstructed defecation. *Diseases of the Colon & Rectum, 42*(2), 223–229.

van Gruting, I. M., Stankiewicz, A., Thakar, R., Santoro, G. A., IntHout, J., & Sultan, A. H. (2021). Imaging modalities for the detection of posterior pelvic floor disorders in women with obstructed defaecation syndrome. *Cochrane Database of Systematic Reviews,* (9), CD011482. https://doi.org/10.1002/14651858.CD011482.pub2

Journal of MEDICINE–24
August 2026, Volume 3, Issue 2, pp. 25−30
DOI: https://doi.org/10.36719/3104-4700/5/25-30

Specific Biochemical Markers in the Early Diagnosis of Connective Tissue Dysplasia in Children

Habiba Gadirli[1*], Tahira Asgarova[2]

Abstract. *Connective tissue disorders, particularly hereditary and secondary collagenoses manifesting during childhood, remain a global health challenge in modern pediatrics and biochemistry. The progression of these pathologies is directly linked to the extensive degradation of the extracellular matrix, which exacerbates mineral metabolism disorders and leads to profound pathological damage at the tissue level. Therefore, the primary objective of this study was to evaluate the role of specific biochemical markers in the early diagnosis of connective tissue dysplasias in children and to comparatively investigate the pathogenetic correlations between the end products of matrix degradation and the mineral-electrolyte profile across various clinical forms. To achieve this, 50 children aged 3–15 years with verified diagnoses were enrolled in the study and divided into two cohorts: the hereditary collagenosis group (n=18) and the secondary (rheumatic) form group (n=22). A control group comprising 10 healthy children was also established. Blood serum samples from all participants were analyzed using biochemical methods to determine the levels of matrix degradation markers, mineral metabolism indicators (Ca, P, Fe), and enzymatic reactivity (ALP). Our findings indicate that disease progression and structural genetic defects significantly accelerate tissue destruction. Notably, a definitive 1.6-fold increase in the levels of specific biochemical markers in the hereditary group compared to the control group demonstrates the intensity of the pathological process. While this intense degradation leads to severe calcium-phosphorus deficiency and a corresponding peak in compensatory bone reactivity in the hereditary group, the rheumatic group is characterized by a sharp decline (1.5-fold) in iron levels. Consequently, the parallel monitoring of these biochemical parameters holds substantial clinical significance for early diagnosis, prognosis, and differential analysis of pathogenetic forms of the disease.*

Keywords: *connective tissue, hydroxyproline, glycosaminoglycans, calcium, phosphorus, iron, alkaline phosphatase, children*

Introduction

Connective Tissue (CT) constitutes approximately 50% of the total body mass in adults, serving as a complex system that regulates structural integrity, trophic, protective, and regenerative functions (Cherkas et al., 2023). Its primary components collagen, elastin and proteoglycans (glycosaminoglycans – GAGs) form the extracellular matrix (Amirrah et al., 2022; Rosa Neto et al., 2024). The degradation of these macromolecular systems triggers severe systemic disorders in children, encompassing both acquired inflammatory and genetic pathologies (Sodhi & Panitch, 2021).

[1]Azerbaijan Medical University, Master's student, Baku, Azerbaijan
[2]Azerbaijan Medical University, Doctor of Biological Sciences, Baku, Azerbaijan
[*]Corresponding author. E-mail: habibaqadirli@gmail.com
Received: 14 April 2026; Accepted: 18 July 2026; Published online: 15 August 2026

In pediatric practice, acute rheumatic fever and juvenile idiopathic arthritis represent significant socio-medical challenges (Carapetis et al., 2016). Acute rheumatic fever is an autoimmune process triggered by Streptococcus pyogenes infection, leading to irreversible sclerotic damage to heart valves (Nigrovic et al., 2018; Sinitskaya et al., 2024; Lorenz et al., 2024). In juvenile idiopathic arthritis, chronic inflammation of the synovial membrane and the activity of enzymes such as matrix metalloproteinase-3 (MMP-3) drive progressive bone-cartilage destruction (Ahn, 2025; Romano et al., 2025; Wojdas et al., 2021).

Alongside acquired inflammatory conditions, hereditary collagenoses such as Marfan syndrome, Ehlers-Danlos syndrome, and osteogenesis imperfecta are prevalent in childhood (Rosa Neto et al., 2024). For instance, fibrillin-1 (FBN1) defects in Marfan syndrome cause hyperactivation of the TGF-β signaling pathway, resulting in multisystem skeletal and cardiovascular complications (Marelli et al., 2023). In Azerbaijan, particularly in southern regions, the high frequency of consanguineous marriages contributes to a significant incidence of these hereditary CT disorders.

Since both hereditary collagenoses and rheumatism often present with similar phenotypic features in their initial stages, differential diagnosis remains a clinical challenge. Therefore, analyzing serum levels of free hydroxyproline (a collagen breakdown product) and total GAGs, alongside mineral-electrolytes (Ca, P, Fe) and alkaline phosphatase (ALP) activity, is essential for accurately identifying the nature and intensity of tissue destruction (Tush et al., 2019). Evaluating this specific biochemical profile holds great scientific and practical significance for the differential diagnosis of hereditary versus secondary connective tissue disorders.

Materials and Methods

The study enrolled a total of 50 children aged 3–15 years, with 40 patients allocated to the main cohort and 10 to the control group. Within the main cohort, 22 children had a verified clinical diagnosis of rheumatism, while 18 presented with hereditary collagenoses. For comparative purposes, a control group consisting of 10 completely healthy children matched for age and sex was included. Blood serum samples obtained from all participants were investigated for ECM degradation markers, mineral profile indicators, and bone-metabolic enzymatic parameters to evaluate tissue metabolism characteristics. To assess the intensity of ECM destruction and the nature of tissue degradation, free hydroxyproline levels in the biological material were quantified spectrophotometrically using a classical method based on a specific color reaction. Concurrently, the concentration of total GAGs, a vital component of the amorphous ground substance of the matrix, was determined via enzyme-linked immunosorbent assay (ELISA) utilizing specific commercial test kits.

To evaluate bone-mineral homeostasis, serum concentrations of calcium (Ca), inorganic phosphorus (P), iron (Fe), and the activity of the alkaline phosphatase (ALP) enzyme were determined colorimetrically on an automated biochemical analyzer. Calcium levels were measured colorimetrically via a specific complex-formation reaction, phosphorus concentration was determined using the ammonium molybdate method, and iron ions were quantified photometrically using the ferrozine reagent. The total activity of ALP, an essential catalytic indicator of bone metabolism and osteoblast function, was determined using a standard colorimetric-kinetic method based on the rate of p-nitrophenyl phosphate (p-NPP) substrate cleavage. All numerical data obtained during the study were processed using SPSS software in compliance with modern statistical principles. The mathematical mean and standard error of the mean were calculated for each biochemical parameter. The statistical significance of intergroup differences was evaluated using the parametric Student's t-test, with results considered statistically reliable and significant at probability thresholds of $p < 0.05$, $p < 0.01$, and $p < 0.001$.

Results

To evaluate the response of core components governing the structural integrity and functional state of connective tissue to pathological processes, the serum dynamics of free hydroxyproline and total GAGs were comprehensively investigated. Immune-inflammatory cascades occurring during the active phase of rheumatism, alongside genetically progressive matrix destruction in hereditary collagenoses, induced sharp deviations in these parameters. The cross-statistical analysis among the three groups and the significance levels of intergroup differences are summarized in Table 1.

Table 1
Comparison of biochemical indicators reflecting tissue metabolism across the study groups

Biochemical markers	Unit	Control group (n = 10)	Rheumatic group (n = 22)	Hereditary collagenopathy group	P
Free hydroxyproline	mkg%	132,5 ± 7,1	182,6 ± 5,4	238,4 ± 6,2	$p_1 < 0,001$ $p_2 < 0,001$ $p_3 < 0,001$
GAG (Glycosaminoglycans)	mg/l	470,0 ± 14,5	712,3 ± 18,2	895,0 ± 22,4	$p_1 < 0,001$ $p_2 < 0,001$ $p_3 < 0,01$

Note. p_1-statistical significance between control and rheumatic groups, p_2-statistical significance between control and hereditary collagenopathy groups, p_3-statistical significance between rheumatic and hereditary collagenopathy groups.

Free hydroxyproline, which reflects the degree of collagen fiber destruction, was measured at 132.5 ± 7.1mkg% in the control group, where as it rose to 182.6 ± 5.4 mkg% in children with rheumatism due to active inflammation. In the hereditary collagenosis group, this indicator increased even more sharply, reaching 238.4 ± 6.2 mkg%. The total GAG concentration, characterizing the state of the extracellular amorphous ground substance, was 470.0 ± 14.5mg/l in healthy children, but increased 1.5-fold to 712.3 ± 18.2 mg/l in rheumatic patients as a result of proteoglycan depolymerization ($P_1 < 0.001$). In the group with hereditary connective tissue dysplasia, GAG levels surged approximately 1.9-fold compared to the control group, reaching a critical threshold of 895.0 ± 22.4 mg/l ($p_2 < 0.001$). The difference between the two diseased groups was also statistically significant ($p_3 < 0.01$).

Connective tissue pathologies are accompanied not only by $_{ECM}$ destruction but also by profound alterations in the body's mineral homeostasis and bone tissue remodeling processes. To evaluate this pathological course at the molecular level, serum calcium (Ca), inorganic phosphorus (P), iron (Fe) levels, and the activity of ALP were studied. The results and intergroup statistical significance levels are summarized in Table 2.

Table 2

Comparison of biochemical indicators reflecting mineral-electrolyte balance across the study groups

Biochemical markers	Unit	Control group (n = 10)	Rheumatic group (n = 22)	Hereditary collagenopathy group	P
Calcium (Ca)	mg/dl	9,15 ± 0,18	8,28 ± 0,16	7,03 ± 0,14	$p_1 < 0,001$ $p_2 < 0,001$ $p_3 < 0,001$
Phosphorus (P)	mg/dl	4,52 ± 0,20	3,84 ± 0,12	3,23 ± 0,11	$p_1 < 0,01$ $p_2 < 0,001$ $p_3 < 0,001$
Iron (Fe)	mkmol/l	15,8 ± 1,1	10,8 ± 0,7	13,4 ± 0,9	$p_1 < 0,001$ $p_2 < 0,001$ $p_3 < 0,05$
Alkaline Phosphatase (ALP)	U/L	215,0 ± 12,5	305,0 ± 14,2	345,0 ± 15,6	$p_1 < 0,001$ $p_2 < 0,001$ $p_3 < 0,05$

Serum calcium and phosphorus levels decreased significantly compared to controls in both rheumatism (Ca: 8.28 ± 0.16 mg/dl; P: 3.84 ± 0.12 mg/dl) and hereditary collagenosis (Ca: 7.03 ± 0.14 mg/dl; P: 3.23 ± 0.11 mg/dl). The most severe bone mineralization defect was recorded in the hereditary collagenosis group ($p_2 < 0.001$). Such a pronounced drop in calcium and phosphorus within the hereditary cohort proves that inorganic components fail to fix properly within a defective collagen matrix. The difference between the two diseased groups was highly significant ($p_3<0.001$). An interesting finding was noted in iron metabolism. Compared to the control group (15.8 ± 1.1 mkmol/l), the iron concentration in children with rheumatism decreased 1.5-fold, dropping to 10.8 ± 0.7 mkmol/l ($p_1<0.001$). This sharp decline is attributed to the sequestration of iron ions with in storage sites during chronic inflammation. In hereditary collagenosis, iron levels decreased only slightly (13.4 ± 0.9 mkmol/l). The difference in iron levels between the two patient groups was statistically significant ($p_3<0.05$). ALP activity, which reflects metabolic stress in bone tissue, was sharply elevated in both cohorts compared to the control (215.0 ± 12.5 U/L). However, the highest enzymatic activity was found in the blood of children with hereditary collagenosis (345.0 ± 15.6 U/L). This biochemical status indicates an increase in the internal functional strain of osteoblasts attempting to compensate for and repair the genetically fragile bone framework. The intergroup difference was mathematically confirmed ($p_3 < 0.05$).

Discussion

The results obtained in this study clearly demonstrate the internal molecular pathogenesis and distinct metabolic profiles of hereditary collagenoses and rheumatism a systemic immune-inflammatory disease whose clinical presentations (joint syndrome, limited mobility, asthenia) sometimes overlap. The status of collagen, the main structural protein of connective tissue, and its surrounding amorphous ground substance determines the rate of tissue metabolism. The serum dynamics of free hydroxyproline, utilized as a specific marker in our study, indicate profound damage in both pathologies, albeit occurring via different pathways. In the rheumatic group, the statistically significant 1.4-fold increase in free hydroxyproline (182.6 ± 5.4 mkg%) relative to controls is directly related to the active immune-inflammatory process ($p<0.001$). Cytokines (IL-1, TNF-α) accumulating in the synovial membranes and joint capsules during rheumatic fever activate matrix metalloproteinases (MMPs) in the extracellular environment. These enzymes degrade mature collagen fibers, causing free hydroxyproline, a product of hydrolysis, to be released into systemic circulation. A completely different scenario is observed in the hereditary collagenosis group, where

free hydroxyproline levels rose 1.8-fold compared to controls, reaching a critical peak of 238.4 ± 6.2 mkg% ($p < 0.001$). In hereditary connective tissue dysplasias, genetic mutations disrupt the initial synthesis of collagen protein, the folding of its triple helix structure, and the molecular cross-linking mechanisms. Being structurally fragile and unstable, these congenital fibers undergo progressive degradation, failing to withstand normal mechanical loads (Nickell et al., 2025).

A similar pathogenetic dependence was tracked in the concentration of GAGs. The 1.5-fold increase in GAGs during rheumatism indicates that the inflammatory process depolymerizes proteoglycan aggregates. In hereditary collagenosis, GAG levels increased 1.9-fold compared to the control group ($p<0.001$). This serves as an essential differential diagnostic criterion proving that genetic defects cause a systemic breakdown of both the fibers and the amorphous zone of the ECM.

A statistically significant decrease in both calcium and inorganic phosphorus levels was recorded in both pathological groups relative to controls. However, the most profound hypocalcemia was noted in the hereditary collagenosis cohort ($p < 0.001$). In hereditary dysplasias, the intrinsic capacity for calcium and phosphorus ion fixation within bone is impaired because the organic matrix is fundamentally defective. In rheumatism, the mineral imbalance is secondary, primarily driven by chronic inflammation activating osteoclasts and accelerating bone resorption.

Iron analysis stands out as another crucial biochemical indicator differentiating the pathogeneses of these two diseases. Iron concentrations dropped sharply to 10.8 ± 0.7 mkmol/l in rheumatic children ($p < 0.001$). This severe hyposideremia is explained by the activation of hepcidin (synthesized in the liver during systemic inflammation), which functionally blocks iron ions within the macrophage system and storage depots. Conversely, in hereditary collagenosis, iron decreased only slightly (13.4 ± 0.9 mkmol/l), pointing to a general microelement imbalance rather than an inflammatory blockade. ALP activity increased sharply in both patient cohorts compared to controls. In rheumatism, this elevation represents a local compensatory response of osteoblasts to inflammation-induced bone-cartilage damage. In the hereditary collagenosis group, the enzyme reached its absolute peak, reflecting internal adaptive strain. The body maximally stimulates the catalytic activity of osteoblastic cells in an effort to rebuild a genetically fragile, defective, and progressively collapsing bone matrix.

Conclusion

Comprehensive biochemical investigations have successfully elucidated the distinct pathogenetic mechanisms of hereditary and acquired connective tissue pathologies in pediatric patients. Matrix destruction observed in hereditary collagenoses is significantly more severe than that seen in rheumatism. The 1.6- to 1.9-fold increase in free hydroxyproline and GAG indicators in the hereditary cohort confirms that tissue structure is systemically dismantled due to genetic factors. While calcium and phosphorus metabolism disorders were apparent in both pathologies, the deep hypocalcemia and hypophosphatemia recorded in hereditary collagenoses are directly linked to the loss of mineralization capacity within the defective collagen matrix. The sharp decline in iron levels during rheumatism uniquely reflects the "functional blockade" mechanism characteristic of chronic inflammation. Conversely, the higher ALP activity in hereditary collagenoses serves as evidence of a maximal compensatory-adaptive process enacted by the body to restore compromised bone tissue. A laboratory panel consisting of free hydroxyproline, GAG, Ca, P, Fe, and ALP parameters is proposed as a highly informative system of differential diagnostic criteria for the early-stage differentiation of hereditary collagenoses from rheumatic lesions.

Declaration of Competing Interests

The authors declare that they have no competing interests.

References

Ahn, J. G. (2020). Role of Biomarkers in Juvenile Idiopathic Arthritis. *Journal of Rheumatic Diseases, 27*(4), 233–240. https://doi.org/10.4078/jrd.2020.27.4.233

Amirrah, N. I., Lokanathan, Y., Zulkifee, I., Wee, M. R., & Fauzi, B. (2022). A Comprehensive Review on Collagen Type I Development of Biomaterials for Tissue Engineering: From Biosynthesis ti Bioscaffold. *Biomedicines, 10*(9), 2307. https://doi.org/10.3390/biomedicines10092307

Carapetis, J. R., Beaton, A., Cunningham, M. W., Guilherme, L., Karthikeyan, G., Mayosi, B. M., & Sable, C. (2016). Acute rheumatic fever and rheumatic heart disease: updates in diagnosis and treatment. *Nature Reviews Disease Primers, 13*(6), 356–368. https://doi.org/10.1038/nrdp.2015.84

Cherkas, O. A., Kobeza, P. A., & Marchenko. (2023). Basic principles of the structure and organization of connective tissue. *Morphologia,* 1, 77–85. https://doi.org/10.26641/1997-9665.2023.1.77-85

Lorenz, N., McGregor, R., Whitcombe, A. L., Sharma, P., Ramiah, C., Middleton, F., Baker, M. G., Martin, W. J., Wilson, N. J., Chung, A. W., & Moreland, N. J. (2024). An acute rheumatic fever immune signature comprising inflammatory markers, IgG3, and Streptococcus pyogenes-specific antibodies. *iScience, 27*(8). https://doi.org/10.1016/j.isci.2024.110558

Marelli, S., Micaglio, E., Taurino, J., Salvi, P., Rurali, E., Perrucci, G. L., Dolci, C., Udugampolage, N. S., Caruso, R., Gentilini, D., Trifiro, G., Callus, E., Frigiola, A., Vincentiis C., Pappone, C., Parati, G., & Pini, A. (2023). Marfan Syndrome: Enhanced Diagnostic Tools and Follow-up Management Strategies. *Diagnostics*, *13*(13), 2284. https://doi.org/10.3390/diagnostics13132284

Nickell, A. L., Erie, T. J., Wold, E. A., Leeuw, A., & Roe, S. J. (2025). Acute Rheumatic Fever. *Academic Pathology, 12*(4). https://doi.org/10.1016/j.acpath.2025.100220

Nigrovic, P. A., Raychaudhuri, S., & Thompson, S. (2018). Review: Genetics and the Classification of Arthritis in Adults and Children. *Arthritis & Rheumatology*, *70*(1), 7–17. https://doi.org/10.1002/art.40350

Romano, F., Scipio, F., Baima, G., Franko, F., Aimetti, M., & Berta, G. N. (2025). Health-Related Quality of Life in Juvenile Idiopathic Arthritis: A Systematic Review of Phase III Clinical Trials. *Journal of Clinical Medicine, 14*(1), 254. https://doi.org/10.3390/jcm14010254

Rosa Neto, N. S., Pereira, I. A., & Azevedo, V. F. (2024). Unraveling the genetic collagen connection: clinical and therapeutic insights on genetic connective tissue disorders. *Advances in Rheumatology*, *64*, 32. https://doi.org/10.1186/s42358-024-00373-z

Sinitskaya, A., Khutornaya, M., Hryachkova, O., Asanov, M., Poddubnyak, A., & Ponasenko, A. (2024). Inflammatory Response Genes' Polymorphism Associated with Risk of Rheumatic Heart Disease. *Journal of Personalized Medicine*, *14*(7), 753. https://doi.org/10.3390/jpm14070753

Sodhi, H., & Panitch, A. (2021). Glycosaminoglycans in tissue engineering: A review. *Biomolecules, 11*(1), 29. https://doi.org/10.3390/biom11010029

Tush, E. V., Eliseeva, T. I., Khaletskaya, O. V., Krasilnikova, S. V., Ovsyannikov, D. Y., Potemina, T. E., & Ignatov, S. K. (2019). Extracellular Matrix Markers and Methods for Their Study. *Modern Tecnologies in Medicine, 11*(2), 133. https://doi.org/10.17691/stm2019.11.2.20

Wojdas, M., Dabkowska, K., & Winsz-Szczotka, K. (2021). Alterations of Extracellular Matrix Components in the Course of Juvenile Idiopathic Arthritis. *Metabolites, 11*(3), 132. https://doi.org/10.3390/metabo11030132

Journal of MEDICINE–24
August 2026, Volume 3, Issue 2, pp. 31−36
DOI: https://doi.org/10.36719/3104-4700/5/31-36

Correlation Between Nitrogenous Waste Products and Prooxidant-Antioxidant System Parameters in Patients with Glomerulonephritis

Maya Gadirova[1*], Firangiz Guliyeva[2]

Abstract. *Chronic kidney diseases, particularly glomerulonephritis (GN), continue to represent a major global public health challenge. The progression of GN is heavily driven by escalating uremic intoxication, which exacerbates oxidative stress and provokes profound cellular pathogenic damage. Consequently, the primary objective of this study was to explore the pathogenetic interactions between end-products of nitrogen metabolism and the prooxidant-antioxidant network across various stages of chronic renal failure in GN patients. To achieve this, a cohort comprising 50 individuals diagnosed with GN (aged 30–80 years), divided into a conservative non-dialysis group (n = 21) and a terminal hemodialysis group (n = 29), along with 10 healthy controls, was recruited. Serum samples from all participants were analyzed using biochemical and spectrophotometric assays to quantify urea and uric acid concentrations, alongside lipid peroxidation (MDA) and antioxidant defense biomarkers (GSH and CAT). Our findings reveal that the advancement of the disease and the deepening of uremic toxicity significantly accelerate oxidative stress, culminating in a severe depletion of antioxidant defense mechanisms during the terminal stage. Therefore, the concurrent monitoring of these biochemical indices holds substantial prognostic value in clinical settings.*

Keywords: *glomerulonephritis, uremic intoxication, urea, oxidative stress, malondialdehyde, catalase, reduced glutathione*

Introduction

Currently, glomerulonephritis (GN) represents a profound global health challenge, serving as a primary driver for the development of chronic kidney disease (CKD) and its end-stage counterpart. Affecting millions worldwide, this pathology consistently ranks among the leading factors contributing to end-stage renal disease (GBD Chronic Kidney Disease Collaboration, 2020; Kramer et al., 2021). As the disease progresses, the deterioration of renal filtration capacity precipitates a pathological accumulation of nitrogenous metabolic end-products in the bloodstream, culminating in severe uremic intoxication (Dounousi et al., 2006).

Fundamental research indicates that the uremic milieu goes beyond the mere mechanical retention of metabolites; it acts as an aggressive pathogenetic trigger for the massive release of free radicals within the body (Himmelfarb et al., 2002; Liakopoulos et al., 2017).

[1]Azerbaijan Medical University, Master's student, Baku, Azerbaijan
[2]Azerbaijan Medical University, PhD in Biology, Baku, Azerbaijan
[*]Corresponding author. E-mail: gadirovamaya3@gmail.com
Received: 8 April 2026; Accepted: 9 July 2026; Published online: 15 August 2026

The chronic inflammatory state and mitochondrial dysfunction inherent to GN lead to the unchecked generation of reactive oxygen species (ROS) and the establishment of severe oxidative stress (Bhatia et al., 2020). Because these radicals primarily target the phospholipid bilayers of cellular membranes, the process of lipid peroxidation (LPO) is acutely accelerated (Manful et al., 2025).

Malondialdehyde (MDA), one of the most toxic terminal products of LPO, is highly reactive and capable of denaturing renal architectures while inducing cellular death (Ayala et al., 2014; Niedernhofer et al., 2003). Concurrently, the pathogenetic involvement of uric acid—a residual product of purine metabolism—warrants particular scientific attention. Although it exhibits antioxidant properties under physiological conditions, the backdrop of uremic hyperuricemia forces uric acid to alter its nature, functioning instead as a potent prooxidant that further exacerbates oxidative injuries (Sautin & Johnson, 2008).

To counteract oxidative damage, the human body mobilizes a sophisticated antioxidant defense network. Reduced glutathione (GSH), the most crucial non-enzymatic component of this system, directly scavenges and neutralizes free radicals; however, its reserves are rapidly exhausted under conditions of chronic stress and inflammation (He & Shi, 2023; Rai et al., 2021). On the other hand, catalase, a fundamental element of the enzymatic defense, shields cells by detoxifying harmful hydrogen peroxide (Aladyeva & Zimatkin, 2022; Hong & Park, 2021).

In light of these dynamics, a comprehensive evaluation of how uremic intoxication impacts oxidative damage and the eventual exhaustion of compensatory mechanisms holds substantial clinical relevance. Such insights are essential not only for unraveling the developmental mechanisms of renal pathologies but also for conceptualizing and designing novel, targeted antioxidant therapeutic strategies.

Materials and Methods

This research enrolled a cohort of 50 patients diagnosed with glomerulonephritis, aged between 30 and 80 years, comprising 27 females (54%) and 23 males (46%). A control group consisting of 10 apparently healthy individuals within a matched age bracket was also included. Based on their clinical status, the patients were stratified into two primary cohorts: the first group consisted of 21 patients in the conservative, non-dialysis stage of the disease, while the second group comprised 29 terminal-stage patients undergoing regular hemodialysis. Blood samples obtained from all participants were utilized to evaluate uremic intoxication markers—serving as indicators of renal functional capacity—alongside parameters of lipid peroxidation (LPO) and the antioxidant defense system (AOS). Serum urea levels were quantified utilizing the classical colorimetric Fearon assay, which relies on a direct chemical interaction with diacetyl monoxime. Conversely, uric acid concentrations were determined via a specific enzymatic uricase-peroxidase (Trinder reaction) colorimetric method.

To ascertain the extent of cellular injury and oxidative stress, LPO and AOS indicators were evaluated using spectrophotometric techniques. The serum concentration of malondialdehyde (MDA), the principal end-product of lipid peroxidation, was measured using the conventional method based on its reaction with thiobarbituric acid (TBA) under elevated temperatures and acidic conditions. For the analysis of antioxidant system elements, the level of reduced glutathione (GSH) was determined colorimetrically through the specific reaction of free sulfhydryl groups with Ellman's reagent (DTNB). Concurrently, catalase enzyme activity was assessed in erythrocyte hemolysates based on the principle of measuring the hydrogen peroxide decomposition rate.

All numerical data acquired during the study were processed using Microsoft Excel software, in accordance with modern biomedical statistical guidelines. For each analyzed biochemical parameter,

the arithmetic mean and its standard error (M ± m) were calculated. The statistical significance of intergroup variances (among the control, conservative, and terminal groups) was evaluated using the parametric Student's t-test, with findings deemed statistically reliable at probability thresholds of $p < 0.05$, $p < 0.01$, and $p < 0.001$. Furthermore, Pearson's correlation analysis (r) was applied to determine the direction and magnitude of the reciprocal associations between uremic intoxication markers, cellular damage indices, and antioxidant defense components.

Results

To evaluate the excretory capacity of the kidneys, the serum concentrations of urea and uric acid were measured in the enrolled glomerulonephritis patients across different stages of disease progression and subsequently compared with those of the healthy control cohort. The resulting quantitative data are summarized in Table 1.

Table 1
Comparative analysis of serum urea and uric acid levels between glomerulonephritis patients at various disease stages and the control group

Parameters	Control group	Conservative group (n = 21)	Terminal group (n = 29)	p-value
Uric acid mg/dL	3,9 ± 0,45	4,5 ± 0,58	7,34 ± 0,65	$p_1 > 0,05$ $p_2 < 0,001$ $p_3 < 0,001$
Urea mM/L	4,6 ± 0,7	15,4 ± 1,8	20,9 ± 2,3	$p_1 < 0,001$ $p_2 < 0,001$ $p_3 < 0,005$

Note. p_1 – significance of the difference between control and conservative groups; p_2 – between control and terminal groups; p_3 – between conservative and terminal groups.

As depicted in Table 1, the levels of nitrogenous metabolic end-products exhibited a significant elevation across both disease stages relative to the control group. Specifically, when compared to healthy subjects, urea concentrations surged by 3.3-fold ($p < 0.001$) in the conservative stage and approached an approximate 4.5-fold increase ($p < 0.001$) in the terminal hemodialysis group. Concurrently, uric acid levels demonstrated a sharp escalation, particularly during the terminal stage, exceeding control values by roughly 1.9-fold ($p < 0.001$).

To evaluate the cellular-level damage inflicted by this deepening uremic intoxication, parameters of lipid peroxidation (MDA) and the antioxidant defense system (GSH, CAT) were thoroughly investigated (Table 2).

Table 2
Intergroup comparative characteristics of LPO and AOS indicators in glomerulonephritis patients according to the disease stage

Parameters	Control group	Conservative group (n = 21)	Terminal group (n = 29)	p-value
MDA (nmol/mL)	2,85 ± 0,11	6,72 ± 0,13	7,91 ± 0,26	$p_1 < 0,001$ $p_2 < 0,001$ $p_3 < 0,001$
GSH (μmol/mL)	0,55 ± 0,026	0,39 ± 0,01	0,405 ± 0,021	$p_1 < 0,001$ $p_2 < 0,01$ $p_3 > 0,05$
CAT (U/mgHb)	18,5 ± 0,9	37,4 ± 2,4	10,7 ± 1,2	$p_1 < 0,001$ $p_2 < 0,001$ $p_3 < 0,001$

One of the most compelling findings of this study involves the dynamic trajectory of intracellular catalase activity. In the conservative stage, a 2.4-fold rise in MDA was accompanied by a compensatory twofold amplification in catalase activity (37.4 ± 2.4 U/mgHb; $p < 0.001$). However, as oxidative stress reached its peak during the terminal stage (MDA – 7.91 ± 0.26 nmol/mL), the antioxidant system underwent severe exhaustion. Consequently, catalase activity plummeted sharply, falling even below the baseline control levels (10.7 ± 1.2 U/mgHb).

To ascertain the direct impact of uremic toxins on the prooxidant-antioxidant balance, a Pearson correlation analysis was conducted among the investigated biochemical markers. The analysis revealed a moderate positive correlation between serum urea concentrations and MDA—the terminal product of lipid peroxidation—in both the non-dialysis conservative group ($r = +0.44$; $p < 0.05$) and the hemodialysis-dependent terminal group ($r = +0.49$; $p < 0.01$). Parallel to this, the elevation in urea was accompanied by a concurrent decline in GSH, the non-enzymatic component of the antioxidant system, across both cohorts ($r = -0.47$; $p < 0.05$ and $r = -0.41$; $p < 0.05$, respectively). Interestingly, the relationship between urea and the enzymatic antioxidant catalase shifted depending on the disease stage: a moderate positive correlation was recorded during the active compensatory phase of the conservative stage ($r = +0.44$; $p < 0.05$), whereas an inverse relationship emerged during the decompensated terminal stage ($r = -0.52$; $p < 0.01$).

Conversely, the associations between uric acid and oxidative stress indicators (MDA, GSH, and CAT) displayed a distinct dynamic. Although certain correlational trends were observed in both the conservative ($r = +0.36$, $r = -0.33$, $r = 0.32$) and terminal stages ($r = +0.31$, $r = -0.29$, $r = -0.33$), these numerical values failed to achieve statistical significance in either cohort ($p > 0.05$). This observation further corroborates that during glomerulonephritis, the primary burden of driving oxidative stress likely falls on other uremic toxins, such as urea, rather than uric acid.

Furthermore, the study evaluated the internal reciprocal dependencies among the elements of the prooxidant and antioxidant systems. The findings demonstrated that in the conservative non-dialysis group, the intensification of lipid peroxidation (MDA) led to a reduction in GSH ($r = -0.44$; $p < 0.05$) while simultaneously exhibiting a moderate positive correlation with CAT activity ($r = +0.46$; $p < 0.05$), indicating a protective cellular response. Nevertheless, this landscape altered drastically in the

terminal hemodialysis group; during this advanced stage, the surge in MDA displayed an inverse relationship with both GSH ($r = -0.52$; $p < 0.01$) and CAT ($r = -0.49$; $p < 0.01$), thereby confirming the complete collapse and exhaustion of the antioxidant defense network.

Discussion

The progression of glomerulonephritis is characterized by a continuous decline in the glomerular filtration rate and the consequent accumulation of nitrogenous metabolic end-products in the body. However, in clinical medicine, the uremic syndrome is recognized not merely as a mechanical retention of metabolites, but rather as a complex pathogenetic process that triggers severe metabolic dysfunctions at the cellular level, notably acute oxidative stress.

Our findings demonstrate that in both the conservative and terminal stages of the disease, the serum concentration of urea—a principal marker of nitrogen metabolism—rises sharply. Concurrently, uric acid levels exhibit an upward trend toward the upper limit in the terminal phase relative to the control group. This intensifying uremic environment induces an excessive generation of reactive oxygen species (ROS) within the organism. The assault of free radicals on the phospholipid bilayer of cell membranes accelerates the lipid peroxidation (LPO) process, a phenomenon corroborated in our study by the statistically significant elevation of MDA levels in both patient cohorts. The robust positive correlation observed between urea and MDA across both the conservative and terminal groups implies that the extent of oxidative damage is directly proportional not solely to urea, but to the overall magnitude of uremic intoxication.

To comprehend the pathogenetic mechanisms of oxidative stress, our most crucial discovery lies in the biphasic antioxidant response mounted by the body against prooxidant attacks. During the conservative stage of the disease, set against the backdrop of accelerated LPO, the nearly twofold amplification of intracellular catalase activity compared to the control group must be interpreted as a robust compensatory-adaptive mechanism. In other words, the cell maximally mobilizes its defensive front to neutralize the surging free radicals and hydrogen peroxide (H_2O_2) toxicity driven by the uremic milieu. This precisely explains the positive correlation registered between catalase, MDA, and urea during the conservative phase, indicating that the organism remains capable of combating oxidative stress. Nevertheless, the concurrent decline in the levels of GSH, a non-enzymatic antioxidant, signifies that these defensive reserves are already being partially depleted.

In the terminal stage, however, the chronicity of the process, the mounting uremic load, and the irreversible damage to renal tissue culminate in the complete collapse—or decompensation—of the antioxidant system. In this phase, alongside the further deepening of LPO, the persistently low levels of GSH coupled with the acute suppression of previously elevated catalase activity to levels below those of the controls, indicate that the system has reached a state of exhaustion. The inversion of the correlation between catalase, MDA, and urea into an inverse relationship within the terminal group serves as the mathematical and clinical proof of this profound antioxidant deficit.

Conclusion

The conducted research establishes that the impairment of renal function and the subsequent accumulation of nitrogenous waste products in patients with glomerulonephritis induce severe oxidative stress within the body. Throughout the developmental dynamics of the disease, the antioxidant defense system initially activates as a compensatory measure; however, it is entirely depleted by the profound impact of uremic intoxication in the terminal stage. The tight correlative links uncovered between the severity of renal failure, lipid peroxidation, and antioxidant indicators underscore that oxidative stress plays a pivotal role in the pathogenesis of chronic kidney diseases. Consequently, incorporating the assessment of the prooxidant-antioxidant status alongside traditional

uremic markers in the routine clinical management and monitoring of glomerulonephritis patients holds tremendous prognostic significance.

Declaration of Competing Interests

The authors declare that they have no competing interests.

References

Aladyeva, T. L., & Zimatkin, S. M. (2022). Cellular catalase: Structure, biogenesis, diversity, functions. *Experimental Biology and Biotechnology*, 1, 12–22. https://doi.org/10.33581/2957-5060-2022-1-12-22

Ayala, A., Muñoz, M. F., & Argüelles, S. (2014). Lipid peroxidation: Production, metabolism, and signaling mechanisms of malondialdehyde and 4-hydroxy-2-nonenal. *Oxidative Medicine and Cellular Longevity*, 360438. https://doi.org/10.1155/2014/360438

Bhatia, D., Capili, A., & Choi, M. E. (2020). Mitochondrial dysfunction in kidney injury, inflammation, and disease: Potential therapeutic approaches. *Kidney Research and Clinical Practice, 39*(3), 244–258. https://doi.org/10.23876/j.krcp.20.082

Dounousi, E., Papavasiliou, E., Makedou, A., et al. (2006). Oxidative stress is progressively enhanced with advancing stages of CKD. A*merican Journal of Kidney Diseases: the official journal of the National Kidney Foundation, 48*(5), 752–760. https://doi.org/10.1053/j.ajkd.2006.08.015

GBD Chronic Kidney Disease Collaboration. (2020). Global, regional, and national burden of chronic kidney disease, 1990–2017: A systematic analysis for the Global Burden of Disease Study 2017. *The Lancet, 395*(10225), 709–733. https://doi.org/10.1016/S0140-6736(20)30045-3

He, L., & Shi, Y. (2023). Reduced glutathione ameliorates acute kidney injury by inhibiting ferroptosis. *Molecular Medicine Reports*, 27, 123. https://doi.org/10.3892/mmr.2023.13011

Himmelfarb, J., Stenvinkel, P., Ikizler, T. A., & Hakim, R. M. (2002). The elephant in uremia: Oxidant stress as a unifying concept of cardiovascular disease in uremia. *Kidney International, 62*(5), 1524–1538. https://doi.org/10.1046/j.1523-1755.2002.00600.x

Hong, Y. A., & Park, C. W. (2021). Catalytic antioxidants in the kidney. *Antioxidants,* 10, 130. https://doi.org/10.3390/antiox10010130

Kramer, A., Pippias, M., Noordzij, M., et al. (2021). The European Renal Association- European Dialysis and Transplant Association (ERA-EDTA) Registry Annual Report 2018; A summary. *Clinical Kidney Journal, 14*(1), 107–123. https://doi.org/10.1093/ckj/sfaa271

Liakopoulos, V., Roumeliotis, S., Gorny, X., Dounousi, E., & Mertens, P. R. (2017). Oxidative stress in hemodialysis patients: A review of the literature. *Oxidative Medicine and Cellular Longevity*, 3081856. https://doi.org/10.1155/2017/3081856

Manful, C. F., Fordjour, E., Subramaniam, D., Sey, A. A., Abbey, L., & Thomas, R. (2025). Antioxidants and reactive oxygen species: Shaping human health and disease outcomes. *International Journal of Molecular Sciences*, 26, 7520. https://doi.org/10.3390/ijms26157520

Niedernhofer, L. J., Daniels, J. S., Rouzer, C. A., Greene, R. E., & Marnett, L. J. (2003). Malondialdehyde, a product of lipid peroxidation, is mutagenic in human cells. *Journal of Biological Chemistry, 278*(33), 31426–31433. https://doi.org/10.1074/jbc.M212549200

Rai, S. R., Bhattacharyya, C., Sarkar, A., Chakraborty, S., Sircar, E., Dutta, S., et al. (2021). Glutathione: Role in oxidative/nitrosative stress, antioxidant defense, and treatments. *ChemistrySelect,* 6, 4566–4590. https://doi.org/10.1002/slct.202100773

Sautin, Y. Y., & Johnson, R. J. (2008). Uric acid: The oxidant-antioxidant paradox. *Nucleosides, Nucleotides & Nucleic Acids, 27*(6), 608–619. https://doi.org/10.1080/15257770802138558

CONTENTS

Signed: 09.08.2026
Online publication: 15.08.2026
Format: 60/84, 1/8
Stock issuance: 8 p.s.
Order: 204

It has been published on aem.az
Address: 19 A.M.Sharifzade,
Yasamal Dist., Baku, Azerbaijan
Phone: +994 50 209 59 68
e-mail: info@aem.az